ORIGINAL ARTICLE

Effects of palbociclib on oral squamous cell carcinoma and the role of *PIK3CA* in conferring resistance

Nur Syafinaz Zainal[1,2], Bernard Kok Bang Lee[1,2], Zheng Wei Wong[1], Iuan Sheau Chin[1], Pei San Yee[1,2], Chai Phei Gan[1], Kein Seong Mun[3], Zainal Ariff Abdul Rahman[2,4], J. Silvio Gutkind[5], Vyomesh Patel[1], Sok Ching Cheong[1,2]

[1]Head and Neck Team, Cancer Research Malaysia, Selangor 47500, Malaysia; [2]Department of Oral & Maxillofacial Clinical Sciences, Faculty of Dentistry, University of Malaya, Kuala Lumpur 50603, Malaysia; [3]Department of Pathology, Faculty of Medicine, University of Malaya, Kuala Lumpur 50603, Malaysia; [4]Oral Cancer Research and Co-ordinating Centre (OCRCC), Faculty of Dentistry, University of Malaya, Kuala Lumpur 50603, Malaysia; [5]Department of Pharmacology, University of California, San Diego 92093-5004, CA, USA

ABSTRACT

Objective: Lack of effective therapies remains a problem in the treatment of oral squamous cell carcinoma (OSCC), especially in patients with advanced tumors. OSCC development is driven by multiple aberrancies within the cell cycle pathway, including amplification of cyclin D1 and loss of p16. Hence, cell cycle inhibitors of the CDK4/6-cyclin D axis are appealing targets for OSCC treatment. Here, we determined the potency of palbociclib and identified genetic features that are associated with the response of palbociclib in OSCC.

Methods: The effect of palbociclib was evaluated in a panel of well-characterized OSCC cell lines by cell proliferation assays and further confirmed by *in vivo* evaluation in xenograft models. *PIK3CA*-mutant isogenic cell lines were used to investigate the effect of *PIK3CA* mutation towards palbociclib response.

Results: We demonstrated that 80% of OSCC cell lines are sensitive to palbociclib at sub-micromolar concentrations. Consistently, palbociclib was effective in controlling tumor growth in mice. We identified that palbociclib-resistant cells harbored mutations in *PIK3CA*. Using isogenic cell lines, we showed that *PIK3CA* mutant cells are less responsive to palbociclib as compared to wild-type cells with concurrent upregulation of CDK2 and cyclin E1 protein levels. We further demonstrated that the combination of a PI3K/mTOR inhibitor (PF-04691502) and palbociclib completely controlled tumor growth in mice.

Conclusions: This study demonstrated the potency of palbociclib in OSCC models and provides a rationale for the inclusion of *PIK3CA* testing in the clinical evaluation of CDK4/6 inhibitors and suggests combination approaches for further clinical studies.

KEYWORDS OSCC; palbociclib; CDK4/6 inhibitors; *PIK3CA*

Introduction

Cancers that begin in the squamous cells lining the mucosal surfaces of the head and neck region, such as the oral cavity, pharynx, larynx, salivary glands, and nasal cavity are collectively termed as head and neck squamous cell carcinoma (HNSCC). In 2012, oral squamous cell carcinoma (OSCC), the most predominant type of HNSCC, accounted for an estimated 300,400 new cases worldwide and was the 8th most common cancer in developing countries preceding leukemia and non-Hodgkin lymphoma[1]. The standard treatments for OSCC used in the past decades include surgery, radiation therapy, and chemotherapy. Despite advances in these treatment modalities to improve survival and locoregional control, the 5-year survival rate remains below 60%[2]. Moreover, about 50% of patients with OSCC present late at stage 3 and 4[3], resulting in a significant drop in their survival rates[4]. In the past decade, the use of targeted therapy in OSCC was previously limited to cetuximab, a humanized antibody inhibiting the epidermal growth factor receptor. However, the clinical benefit of cetuximab with chemotherapy is moderate, with only 2.7 months improvement in overall survival as compared to chemotherapy alone[5]. Cetuximab treatment is challenged by primary and acquired resistance in patients with OSCC[6]. More recently, the immune checkpoint inhibitors, pembrolizumab and nivolumab, were approved for the treatment of OSCC, but the efficacy of immunotherapy is

only seen in less than 20% of patients[7]. It is apparent that the treatment options for patients with OSCC are currently limited, especially, for patients with advanced disease and who are refractory to chemotherapy, underscoring the unmet need to increase effective treatment options for such patients.

As OSCC is largely driven by several molecular changes affecting the cell cycle, such as amplification of cyclin D1 and loss of p16[8], we investigated if the cell cycle inhibitor, palbociclib, would be effective in treating OSCC. Palbociclib is a specific CDK4/6 inhibitor and the first of its class to be approved for breast cancer in combination with letrozole[9] and fulvestrant[10]. In OSCC, the use of palbociclib in combination with cetuximab is still under clinical investigation[11] and preclinical data evaluating palbociclib are currently limited. Here, we demonstrate the effect of palbociclib on a panel of well-characterized OSCC cell lines and subcutaneous xenograft models. Using genomic information of these well-characterized models, we seek to identify molecular aberrancies that could modulate the response of OSCC to palbociclib, thereby defining new precision therapeutic options for this aggressive malignancy.

Materials and methods

Chemical reagents

Palbociclib was purchased from LC Laboratories (MA, USA). Ribociclib, abemaciclib, and PF-04691502 were purchased from Selleckchem (TX, USA). For *in vitro* use, all reagents were dissolved in 10 mM stocks (palbociclib and PF-04691502 in DMSO, ribociclib and abemaciclib in water) and kept as small aliquots in –20°C until further use. For *in vivo* experiments, palbociclib and PF-04691502 were dissolved in 133 mg/mL and 25 mg/mL stocks, respectively, in DMSO and stored at –20°C until further use.

Cell lines

The ORL series used in this study was established from patients with oral cancer as previously reported[12, 13]. All ORL cell lines were cultured in Dulbecco's modified Eagle's medium/Nutrient mixture F12-Ham's medium (DMEM/F12; Hyclone, UT, USA) supplemented with 10% (v/v) heat-inactivated fetal bovine serum (FBS; Gibco, Auckland, NZ) and 500 ng/mL of hydrocortisone (Sigma-Aldrich, MO, USA). Generation of CAL27/*PIK3CA*[H1047R+] was described previously[14]. CAL27, CAL27/*PIK3CA*[H1047R+] and MCF-7 cells were grown in DMEM (Gibco, Auckland, NZ) supplemented with 10% (v/v) heat-inactivated FBS. All cell lines have been authenticated to tissues and/or blood from corresponding patients as described previously[12]. Cells were cultured at 37 °C in a 5% CO_2 humidified atmosphere.

Crystal violet cytostatic assay

The cytostatic effect of palbociclib on a panel of OSCC lines was determined by crystal violet cytostatic assay. Briefly, 8×10^3 cells were seeded in triplicates in 12-well plates and following overnight incubation, cells were exposed to palbociclib at concentrations ranging from 0.008–2 μM or vehicle control [0.5% (v/v) DMSO]. After 72 h of incubation, crystal violet solution consisting of 2% (w/v) crystal violet (Sigma Aldrich, MO, USA), 10% (v/v) formaldehyde (Merck Millipore, MA, USA), and distilled water was added into each well and the plates were further incubated for an additional 10 min with agitation. The crystal violet solution was then removed from each well and cells were washed 2 times with water and dried overnight. The following day, the resulting crystals were dissolved in 500 μL of DMSO and the absorbance was measured at 590 nm using a Synergy H1 Multi-Mode reader (BioTek Instruments, VT, USA). The concentration of drug required to cause 50% reduction in cell growth was calculated as $GI_{50} = [(Abs_p - Abs_0)/(Abs_{DMSO} - Abs_0)] \times 100\%$, where Abs_0 is the absorbance value of untreated cells at day 0, and Abs_p and Abs_{DMSO} are the absorbance values of palbociclib-treated and VC-treated cells after 72 h, respectively.

Click-iT EdU cell proliferation assay

Cell proliferation was determined by the Click-iT EdU assay (Invitrogen, CA, USA) following the manufacturer's instructions. Briefly, 7×10^4 cells per well were grown overnight on glass coverslips and treated with 0.06–0.5 μM palbociclib or 0.5% (v/v) DMSO for 24 h. Cells were incubated with 10 μM 5-ethynyl-2′-deoxyuridine (EdU) for 2–6 h prior to fixation with 3.7% (v/v) formaldehyde. The cells were permeabilized with 0.1% (v/v) Triton X-100 in phosphate buffer, followed by EdU detection *via* a copper-catalyzed reaction and nuclei staining by Hoechst 33342. The coverslips were then mounted on glass slides using VECTASHIELD® Mounting Medium (Vector Laboratories, Burlingame, CA, USA). Slides were examined on an upright Olympus IX71 microscope (Olympus, Japan) with double bandpass filters to detect fluorescent-stained nuclei (Hoechst 33342-excitation 360–370 nm and emission 420 nm) and

Alexa-labeled EdU (Alexa 647: excitation 650 nm and emission 667 nm). Images were captured from 10 randomly chosen fields of each experiment and analyzed with the QuickCount® software. The number of EdU-positive cells and Hoechst 33342-stained cells was counted and the percentage of EdU-positive cells was calculated (from three independent experiments) using the following formula: number of EdU positive cells/number of Hoechst 33342-stained cells $\times$ 100. EdU-positive cells broadly represent cells that are undergoing DNA synthesis, whereas Hoechst 33342-stained cells represent all cells in the same field.

Cell cycle assay

Briefly, 7×10^4 cells were seeded per well in 12-well plates and treated with 0.06–0.5 μM palbociclib or 0.5% (v/v) DMSO on the following day for 24 h. All floating and attached cells were harvested and fixed in 70% (v/v) ethanol for 16 h at –20°C. Prior to analysis, fixed cells were pelleted and washed in cold phosphate buffered saline, followed by staining with 10 μg/mL propidium iodide solution containing 20 μg/mL RNase for 30 min at 21°C in the dark. Stained cells were analyzed by BD FACSCanto II™ flow cytometer (BD Biosciences, MA, USA) with 10, 000 events collected for each reading. The distribution of DNA in different phases was determined using the ModFit software (Verity Software House, USA). The percentage of cells in each phase was calculated from three independent experiments.

Western blot

Palbociclib (0.06–0.5 μM)-treated and 0.5% (v/v) DMSO-treated cells were lysed on ice in lysis buffer [5 M NaCl, 10% (v/v) NP-40, 1 M Tris pH 8.0, and 0.5 mM DTT] supplemented with HALT protease and phosphatase inhibitor cocktail (Pierce Biotechnology, IL, USA). Cell lysates were then centrifuged at 13,000 $\times$ *g* for 10 min at 4°C prior to estimation of protein content using the BCA method (Thermo Fisher Scientific, MA, USA). For Western blot analysis, 30 μg of total cellular proteins was resolved on a 12% (w/v) sodium dodecyl sulfate-polyacrylamide gel and electrotransferred onto Immobilon-P membrane (PVDF; Millipore, MA, USA) at 100 V for 1.5 h on ice. Membranes were blocked with 5% (v/v) skimmed milk in Tris-buffered saline with 0.1% (v/v) Tween 20 (TBST; Sigma-Aldrich, MO, USA) for 1 h and then probed overnight at 4°C with the indicated primary antibodies at 1:1000 dilution in 1% (v/v)

bovine serum albumin in TBST [pRb (S780), pRb (S795), total Rb1, cyclin D1, cyclin E1, CDK2, CDK4, CDK6, pAKT (S473), total AKT1, pS6, total S6 (Cell Signaling Technology, MA, USA), and α-tubulin (Sigma-Aldrich, MO, USA)]. Next, membranes were washed 3 times in TBST for 5 min each. Membranes were then incubated with the corresponding horseradish peroxidase (HRP)-conjugated secondary antibodies (Southern Biotech, AL, USA) at 1:10,000 dilution in 5% (v/v) skimmed milk in TBST for 1 h at room temperature. This was followed by 3 washes in TBST prior to detection by WesternBright Quantum HRP substrate (Advansta Inc., CA, USA) and visualization using the FluorChem™ HD2 imaging system (ProteinSimple, CA, USA).

In vivo mouse experiments

Six-week-old female NOD/SCID mice were subcutaneously implanted with 2×10^6 cells in both flanks. When the tumors reached the size of approximately 100–200 mm³, the mice were randomized into experimental groups: vehicle control (VC), palbociclib (150 mg/kg body weight, suspended in DMSO 5% and Cremophor-EL 10%, 500 μl p.o), or PF-04691502 (10 mg/kg body weight, suspended in DMSO 4% and 0.5% methylcellulose, 200 μL p.o). Treatment was administered daily by oral gavage for 21 days and tumor measurements were taken using a digital calliper every 3–4 days throughout the experiment. Tumor volumes (V) were calculated as V = ½ length $\times$ (width)². Growth curves were plotted as an average tumor volume of each experimental group against the set time points. At the end of experiment, mice were sacrificed and tumors were harvested for tissue processing and histopathological analysis. All procedures involved in the animal study were reviewed and approved by the Animal Ethics Committee of Universiti Kebangsaan Malaysia (Approval No. CARIF/2016/CHEONG/18-MAY/762-JUNE-2016-JUNE-2019).

Statistical analysis

All data are expressed as mean ± standard deviation (SD) from three independent experiments unless stated otherwise. Statistical analysis was performed using IBM SPSS Statistics for Windows, version 21.0 (IBM Corp., NY, USA). Significant differences between groups were analyzed using 2-tailed independent *t*-test or one-way analysis of variance (ANOVA). A *P*-value less than 0.05 was considered statistically significant.

Results

Palbociclib inhibits the growth of OSCC cells in culture

To examine the effect of palbociclib on OSCC, we treated a panel of OSCC cell lines with 0–2 μM of palbociclib for 72 h. Among the 16 OSCC cell lines tested, 13 were sensitive to palbociclib with a GI_{50} (concentration for 50% of maximal inhibition of cell growth) of less than 1 μM, while three lines with a GI_{50} of more than 1 μM indicated resistance to palbociclib based on the cytostatic assay (**Figure 1A**). The sensitive and resistant groups were significantly different from each other with ~5-fold differences in average GI_{50} values ($P < 0.01$). To further validate the inhibitory effect of palbociclib on cell proliferation, we performed Click-iT EdU proliferative assay on representative palbociclib-sensitive cells (CAL27 and ORL-48) and palbociclib-resistant cells (ORL-150 and ORL-115). Relative to the VC group, palbociclib treatment (0.06 to 0.5 μM) for 24 h reduced the number of EdU-positive cells (represented as red stained-cells) in CAL27 and ORL-48 cells (**Figure 1B**), suggesting a decrease in DNA synthesis activity and blockade of cell cycle progression from G_1 to S phase. As expected, the reduction in EdU-positive cells was not as pronounced in ORL-150 and ORL-115 cells where the reduction in dividing cells was less than 50% even at the highest drug concentration (**Figure 1B** and **1C**).

Anti-proliferative activity of palbociclib is due to G_1 cell cycle arrest

As a selective inhibitor of CDK4/6, palbociclib is known to prevent the initiation of S phase of the cell cycle. To confirm this, we next investigated the anti-proliferative effect of palbociclib through cell cycle analysis following propidium iodide staining in palbociclib-sensitive CAL27 and ORL-48 cells. The cells were treated with palbociclib (0.06 to 0.5 μM) for 24 h. Palbociclib treatment increased the percentage of cells in the G_0/G_1 phase, and concurrently reduced the percentage of S phase cells in a dose-dependent manner for both cell lines (**Figure 1D**). This indicates the inhibition of S phase initiation by palbociclib, which resulted in the arrest of cell cycle progression at the G_0/G_1 phase in OSCC cells. Palbociclib did not induce death in CAL27 and ORL-48 cells as seen by the constant level of cell population in the sub-G_1 phase across the different treatment doses (**Supplementary Figure S1**).

Palbociclib reduces Rb protein levels and phosphorylation

We further investigated the biochemical effect of palbociclib on proteins involved in the Rb pathway, which is critical in regulating the initiation of DNA replication. We first performed a dose-dependent protein expression analysis on palbociclib-sensitive (CAL27 and ORL-48) and palbociclib-resistant cells (ORL-150 and ORL-115) for Rb phosphorylation at S780, S795, and S807/811 as these sites are known to be phosphorylated by CDK4/6[15]. We observed that treatment with palbociclib, especially at 0.5 μM, reduced Rb phosphorylation at all three phosphorylation sites in CAL27, ORL-48, and ORL-150 cells (**Figure 1E**), indicating the blockage of cell cycle progression upon palbociclib treatment. In contrast, ORL-115 cells retained the expression and phosphorylation of Rb at all doses tested (0.06–0.5 μM), validating the resistance of this cell line towards palbociclib, as shown in the proliferative assays described above. As the greatest effect of Rb dephosphorylation was observed at 0.5 μM dose, this concentration was used to conduct a time-dependent protein expression analysis of palbociclib-sensitive cells (CAL27 and ORL-48). Complete dephosphorylation of Rb was observed after 24 h of palbociclib treatment, particularly at S780 and S795 (**Figure 1F**). Additionally, palbociclib steadily downregulated the expression levels of Rb in a time-dependent manner, culminating in low Rb expression at 24 h after treatment in both cell lines. We also noted that the protein levels of cyclin D1, CDK4, and CDK6 were slightly increased with time as a result of palbociclib treatment, consistent with observations in other studies on breast and colorectal cancers[16,17].

Palbociclib inhibits tumor growth in subcutaneous xenograft model

As demonstrated earlier, palbociclib exerted potent inhibitory effect on OSCC cell growth *in vitro*. Next, we investigated *in vivo* efficacy of palbociclib in subcutaneous xenograft models using CAL27 and ORL-48 cells. Mice were randomized to receive either 150 mg/kg of palbociclib or VC when tumors reached an average volume of 100–150 mm³. We observed that palbociclib treatment for 21 days significantly inhibited the growth of CAL27 (VC: 477.5 ± 101.2 mm³ *vs.* palbociclib: 159.76 ± 22.6 mm³; $P = 0.007$) and ORL-48 (VC: 755.06 ± 51.07 mm³ *vs.* palbociclib: 68.47 ± 15.07 mm³, $P = 1 \times 10^{-7}$) xenograft tumors (**Figure 2A** and **2B**). Next, we investigated the expression and phosphorylation of Rb protein in xenograft tumors that were
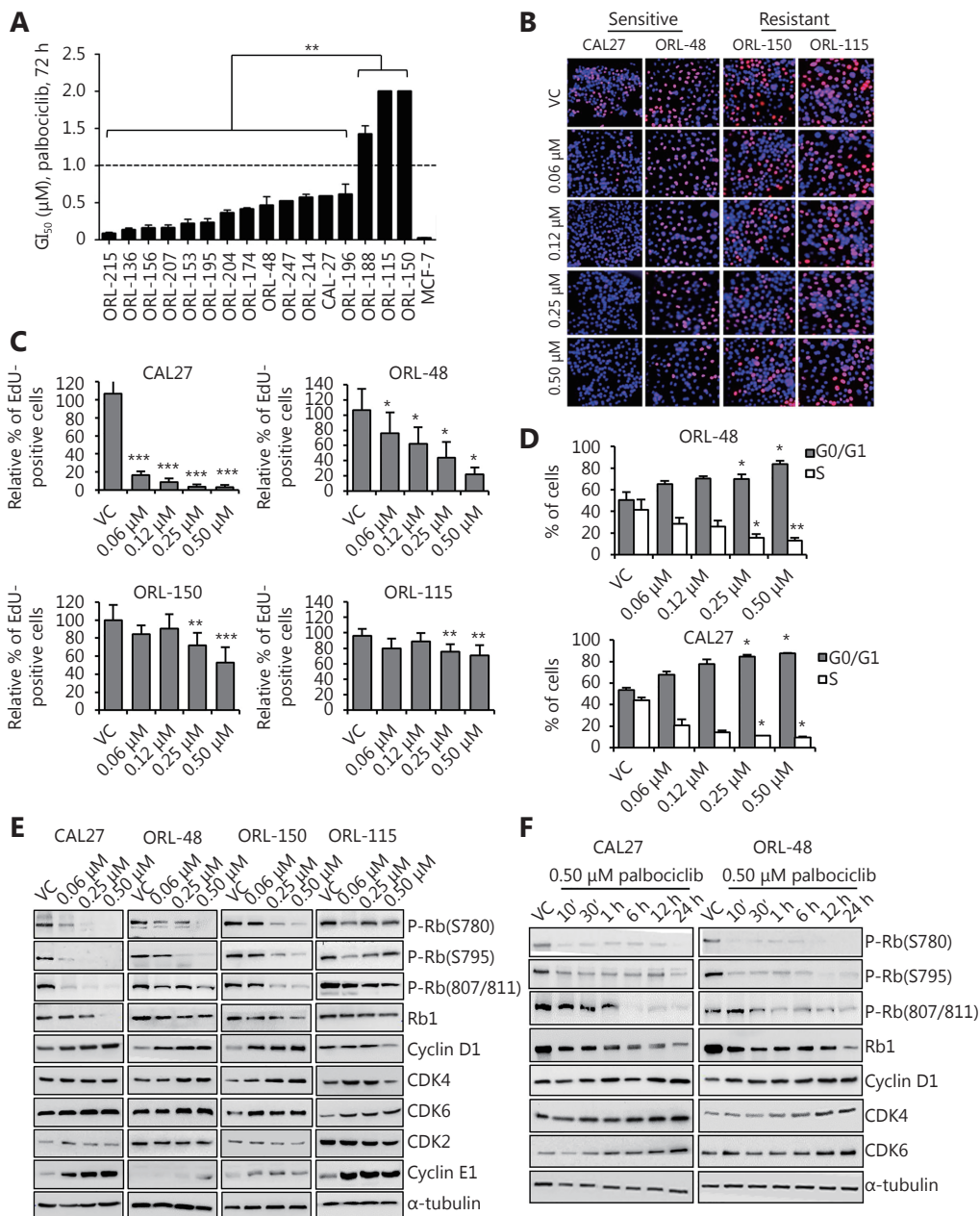
Figure 1 Majority of OSCC cell lines were sensitive to palbociclib. (A) Crystal violet cytostatic assay performed on a panel of OSCC cell lines showed GI_{50} of less than 1 μM in 80% of the cell lines tested, while three lines (ORL-188, ORL-150 and ORL-115) indicated resistance ($GI_{50} > 1$ μM). Cell lines were treated with 72h of 0.008 to 2 μM of palbociclib. (B,C) Cytostatic effect of palbociclib was validated in representative sensitive and resistant cell lines using Click-iT EdU assay. Blue (Hoecsht 33342) represents the total number of cells in any field and red (Alexa 647) represents proliferating cells that have incorporated the EdU label. Palbociclib (24 h) exhibits anti-proliferative effects on CAL27 and ORL-48 as demonstrated by the reduction in the percentage of EdU-positive cells which represents actively dividing cells, but not observed in ORL-115. (D) Escalating dose of palbociclib (24 h) increased G_0/G_1 cell population in CAL27 and ORL-48 cells by propidium iodide analysis. (E) Dose-dependent Western blot analysis of palbociclib showed reduction of Rb phosphorylation (greatest at 0.5 μM) on CAL27, ORL-48 and ORL-150 but not on ORL-115. Cells were treated with the indicated concentrations for 24 h. (F) Time-dependent Western blot analysis on sensitive cells indicated reduction of Rb phosphorylation within 24 h at 0.5 μM palbociclib treatment. Symbols *, ** and *** denote $P < 0.05$, $P < 0.01$, $P < 0.001$, respectively. Western blot results shown are representative of at least two independent experiments.
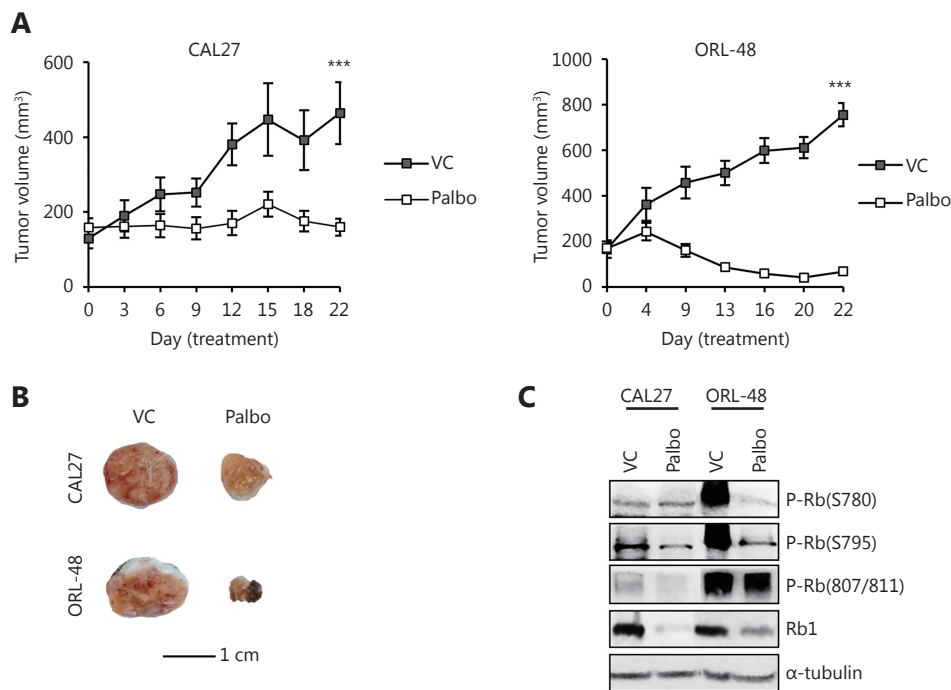
Figure 2 Palbociclib controls OSCC xenograft tumors. (A) Mice bearing CAL27 and ORL-48 xenograft tumors were treated with either vehicle control (VC) or 150 mg/kg palbociclib (Palbo) for 21 d. Palbociclib significantly inhibited growth of OSCC subcutaneous xenograft ORL-48 and CAL27 tumors. Results shown are mean ± SEM (n = 10 tumors per group). Symbol *** denotes P < 0.001. (B) Representative tumors harvested at the end of treatment showed decreased tumor volume in the palbociclib treatment group. (C) Western blot analysis on proteins extracted from tumors at end-point showed palbociclib treatment reduced Rb phosphorylation in mouse tumors particularly at S780 and S795 phosphorylation sites.

harvested at the end of the study. As shown in **Figure 2C**, palbociclib treatment resulted in the reduction in Rb phosphorylation at S795 in CAL27 xenograft tumors. The effect was more apparent in ORL-48 xenograft tumors, wherein reduction in Rb phosphorylation was observed at both S780 and S795 sites, consistent with the observation that tumor volume control was more significant in this cell line compared to that in CAL27 cells (**Figure 2A** and **2B**). Although we observed marked reduction in Rb phosphorylation at S780 and S795, Rb phosphorylation was not affected at S807/811 (**Figure 2C**), which was consistent with *in vitro* observations for ORL-48 (**Figure 1E**). In addition, palbociclib treatment caused reduction in the total Rb levels of both CAL27 and ORL-48 tumors, consistent with that observed *in vitro*. These observations confirmed that palbociclib inhibited the CDK4/6-Rb pathway, which eventually led to tumor control in mice.

Cancer cells harboring *PIK3CA* mutation are less responsive to palbociclib

From our data, we observed that a subset of OSCC cell lines was resistant to palbociclib. We investigated whether certain genetic features could lead to palbociclib resistance. To achieve this, we compared the mutational profiles of palbociclib-sensitive and -resistant cell lines as determined by cytostatic assay in **Figure 1A**. We found that two out of three cell line in the resistant group carried mutations in *PIK3CA* (H1047L and Q546R in ORL-115 and ORL-150, respectively)[12,18], while none of the palbociclib-sensitive cell lines had any mutations in this gene (P < 0.001; **Figure 3A**). This observation was validated with a larger data set from Genomics of Drug Sensitivity in Cancer (GDSC) comprising of 789 palbociclib-treated cancer cell lines of all available cancer types in the database. These cell lines were grouped based on their *PIK3CA* mutational status [wild-type (WT) or having any mutations in *PIK3CA*] and their geometric means of IC_{50} were compared. Cancer cells having mutation in *PIK3CA* have a higher geometric mean IC_{50}, implying that they are more resistant to palbociclib compared to cell lines with WT *PIK3CA*; however, the difference was not statistically significant (P = 0.101; **Figure 3B**). This led us to further investigate the role of *PIK3CA* mutations in conferring palbociclib resistance in OSCC.
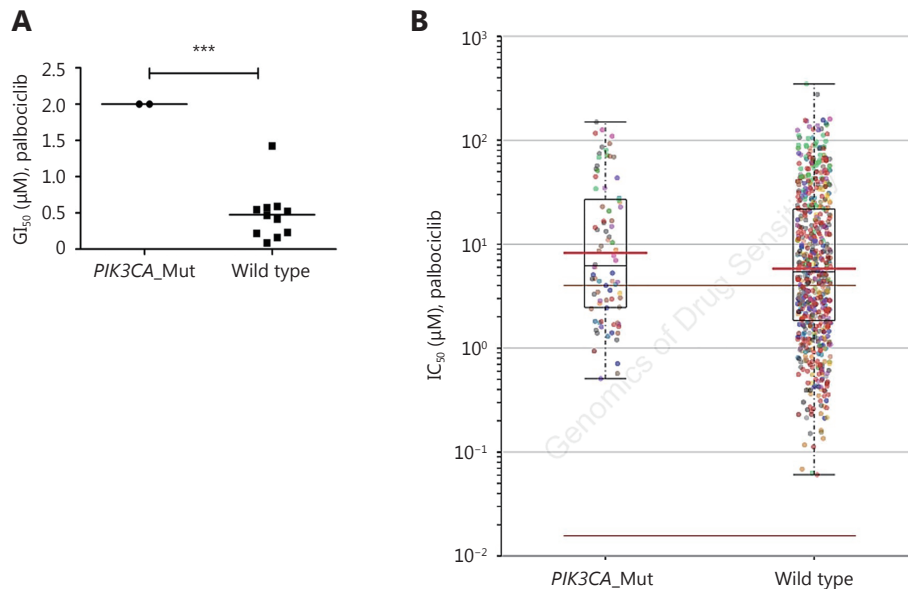
Figure 3 Palbociclib-resistant cell lines harbour *PIK3CA* mutation. (A) Comparison of the mutational status between sensitive and resistant cells obtained from the cytostatic data of **Figure 1A** revealed significant association of *PIK3CA* mutation with palbociclib resistance. Symbol *** denotes $P < 0.001$. (B) According to Genomics of Drug Sensitivity in Cancer (GDSC) database, cancer cells having any mutation in the *PIK3CA* gene have higher geometric mean IC_{50}, implying them to be more resistant to palbociclib compared to wild-type cancer cells. A total number of 789 palbociclib-treated cancer cell lines of all available cancer types are included in the analysis.

PIK3CA mutation decreases response to palbociclib

To test whether *PIK3CA* mutations confer resistance to palbociclib in OSCC, we used CAL27 cells that were previously retro-engineered to stably express $PIK3CA^{H1047R}$ alteration[14]. The mutational status of *PIK3CA* in isogenic (mutant and WT) CAL27 cell lines was verified by Sanger sequencing, where the mutant CAL27 cells have base substitution from A (WT) to G, resulting in the replacement of histidine (H) with arginine (R) at position 1047 (**Supplementary Figure S2A**). The presence of the H1047R mutation was also confirmed by western blotting, wherein increased Akt phosphorylation was observed in mutant cells (**Supplementary Figure S2B**).

The differential sensitivity to palbociclib in these isogenic cells was first evaluated by EdU proliferation assay. The inhibition of cell proliferation was more pronounced in WT cells as the percentage of EdU-positive cells was observed to be lower by ~4-fold compared to that in *PIK3CA* mutant cells at a dose of 0.5 μM ($P < 0.001$; **Figure 4A** and **4B**). In addition, we assessed whether the presence of *PIK3CA* mutation would affect the response to two other clinically approved CDK4/6 inhibitors[19,20]. We treated isogenic CAL27 cells with ribociclib and abemaciclib (0.25–0.5 μM) and

found that the number of EdU-positive cells was also significantly lower in WT cells as compared to that in *PIK3CA* mutant cells (**Figure 4C**). These results indicated that the presence of *PIK3CA* mutation reduced the sensitivity of CAL27 to CDK4/6 inhibitors, and this observation was not restricted to palbociclib.

Next, flow cytometry was performed to evaluate the differences in G_1 cell cycle arrest in the respective WT and mutant cells. As demonstrated previously, palbociclib treatment arrests cells at the G_0/G_1 phase. As shown in **Figure 4D**, the percentage of cells in the G_0/G_1 phase for *PIK3CA* mutant cell line was lower than that for WT cells at all doses tested, with statistical significance at 0.5 μM palbociclib ($P = 0.02$). Concurrently, *PIK3CA* mutant cell lines showed greater percentage of cells in the S phase than WT cells at 0.5 μM treatment dose ($P = 0.03$), indicating higher cell cycle activity, consistent with the results of palbociclib resistance.

PIK3CA mutant cells escape CDK4/6 inhibition *via* the CDK2 pathway

To investigate the biochemical mechanism that caused *PIK3CA* mutant cells to exhibit higher resistance to palbociclib, proteins were extracted from the isogenic cells
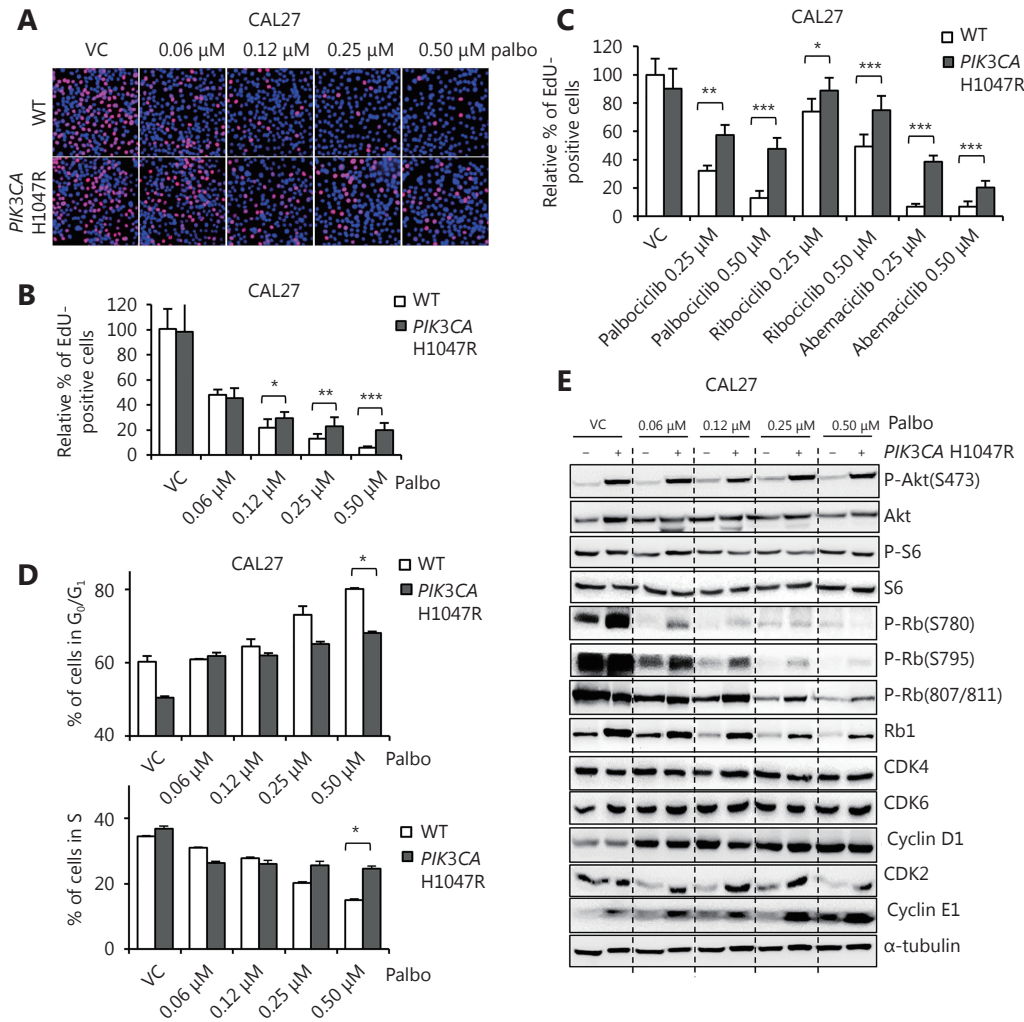
Figure 4 *PIK3CA*-mutant cells were less inhibited by palbociclib. (A, B) Less inhibition by palbociclib (24 h) was observed in *PIK3CA*-mutated CAL27 cells as indicated by the increased percentage of dividing cells as compared to WT by Click-iT EdU assay. Blue (Hoechst 33342) represents the total number of cells in any field and red (Alexa 647) represents proliferating cells that have incorporated the EdU label. (C) *PIK3CA*-mutated CAL27 cells were less sensitive to all available specific CDK4/6 inhibitors (palbociclib, ribociclib and abemaciclib) at 0.25 and 0.5 μM by Click-iT EdU assay. (D) Reduced G_0/G_1 and increased S phase population were seen in *PIK3CA*-mutated cells as compared to WT by cell cycle (propidium iodide) analysis, following 24 h palbociclib treatment. (E) Western blot analysis showed less reduction of Rb phosphorylation and expression in *PIK3CA*-mutated cells as compared to WT upon 24 h palbociclib treatment. Increased expressions of CDK2 and Cyclin E1, but no changes in CDK4, CDK6 and cyclin D1 suggested S phase entry through CDK2/cyclin E complexes in *PIK3CA*-mutated cells. Symbols *, ** and *** denote $P < 0.05$, $P < 0.01$, and $P < 0.001$ respectively. Western blot results shown are representative of at least two independent experiments.

after 24 h of treatment with escalating doses of palbociclib (0.06 to 0.5 μM), and proteins within the Akt and Rb pathway were examined by Western blot (**Figure 4E**). Due to the presence of the *PIK3CA*[H1047R] mutation, mutant cells showed significantly higher phosphorylation of Akt as compared to WT cells across all palbociclib doses tested. The reduction in Rb phosphorylation, particularly at S795 and S807/811, was not as marked in *PIK3CA* mutant cells treated

with palbociclib as compared to that in WT cells. Less reduction in Rb phosphorylation at the S780 site was also detected; however, it was only apparent at the 0.06 μM treatment dose. Lack of reduction in Rb phosphorylation at S807/811 and S795, but clear reduction at S780 in the *PIK3CA* mutant cells suggested an S phase entry through phosphorylation of Rb by the CDK2/cyclin E1 complex[15,21,22]. We noted that palbociclib treatment (0.06 to 0.5 μM) caused
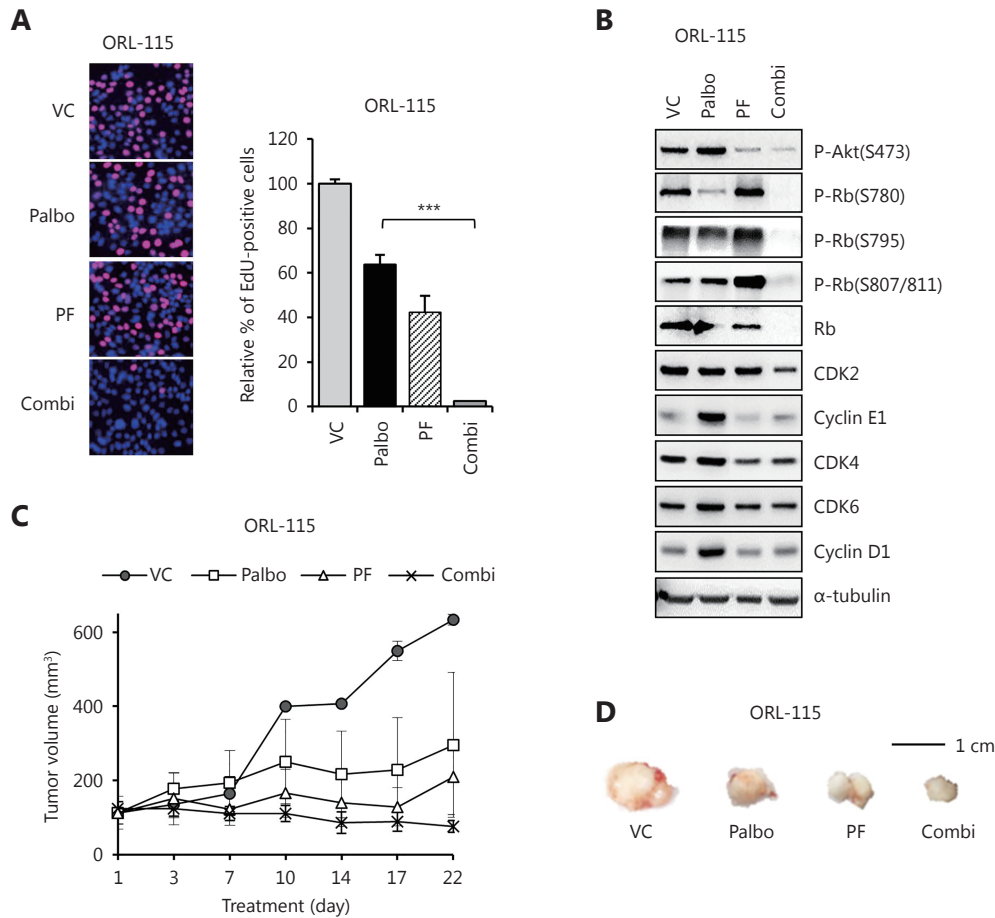
Figure 5 Palbociclib-resistant cell line was re-sensitized when co-inhibited with a PI3K/mTOR inhibitor. (A) From Click-iT EdU assay, ORL-115 (naturally carrying a H1047L *PIK3CA* mutation) cells showed resistance to 0.5 µM palbociclib (24 h) in relative to CAL27 WT cells. Combining the treatment with 0.25 µM PF-04691502 (a PI3K/mTOR inhibitor) significantly improved growth inhibition in ORL-115 cells. Symbol *** denotes $P < 0.001$. (B) Western blot analysis of proteins extracted from ORL-115 cells treated with 0.5 µM palbociclib and 0.25 µM PF-04691502 (24 h) showed non-phosphorylated Rb and prevention of cell cycle kinases upregulations. (C) Mice bearing ORL-115 xenograft tumor were treated with either VC, palbociclib (150 mg/kg), PF-04691502 (10 mg/kg), or combination of both for 21 d. Only the combination treatment resulted in the gradual decrease of tumor volumes. Results shown are mean ± SEM (n = 10 tumors per group). (D) Representative ORL-115 xenograft tumor harvested at the end of experiment showed the greatest tumor inhibition from the combination group.

reduction in CDK2 expression in WT cells, however CDK2 expression was sustained throughout the range of palbociclib dose tested in the mutant cells. Cyclin E1, which partners with CDK2 to phosphorylate Rb, showed increased levels of expression in the mutant cells as compared to those in WT cells when palbociclib treatment was given. On the contrary, we did not see any changes in CDK4, CDK6, and cyclin D1 protein levels between WT and mutant cells across all treatment doses, suggesting that the CDK2/cyclin E1 pathway is a potentially compensatory pathway that led to Rb phosphorylation in *PIK3CA* mutant cells, resulting in an escape from palbociclib treatment.

Combination of CDK4/6 and PI3K inhibitors sensitizes the *PIK3CA* mutant cell line ORL-115

Since *PIK3CA* mutations confer resistance to palbociclib, we used the inherently resistant cell line ORL-115 to determine whether *PIK3CA* mutant cells could be sensitized to palbociclib with a combination treatment targeting the PI3K pathway. Using ORL-115, which harbors the *PIK3CA*[H1047L] mutation, we showed that treatment with a combination of palbociclib and a PI3K/mTOR inhibitor (PF-04691502) substantially increased sensitivity to palbociclib, where the

lowest percentage of EdU-positive cells was observed in the combination group (**Figure 5A**). Consistent results were observed for ORL-150 (data not shown). The Western blot results in ORL-115 cells indicated that treatment with palbociclib alone resulted in the upregulation of cyclin E1 and sustained levels of CDK2, possibly leading to Rb phosphorylation especially at S795 and S807/811 sites (**Figure 5B**). Inhibiting both CDK4/6 and PI3K pathways prevented the upregulation of cyclin E1, reduced CDK2 levels, and resulted in the accumulation of non-phosphorylated Rb at all three sites, suggesting improved growth inhibition in ORL-115 cells. Additionally, co-treatment with PF-04691502 resulted in the reduction in levels of other cell cycle kinases, such as CDK4, CDK6, and cyclin D1 as compared to palbociclib treatment alone. Consistently, *in vivo*, we demonstrated that ORL-115 cells were less responsive to palbociclib, as sustained tumor growth was still observed in animals treated with palbociclib, with tumor volume steadily increasing from 112 mm^3 (day 1) to 296 mm^3 (day 22) throughout the treatment period (**Figure 5C**). Only when the combined treatment was given, a sustained tumor volume reduction was achieved from 124 mm^3 (day 1) to 76 mm^3 (day 22). ORL-115 tumors that were treated with PF-04691502 also demonstrated better tumor growth control compared to those treated with palbociclib; however, this was not as marked as compared to the combination treatment of palbociclib and PF-04691502 (**Figure 5C** and **5D**).

Discussion

Alterations within the cell cycle machinery are common molecular alterations found in HNSCC, including mutations in *TP53* (74%), loss of p16 (49%), and amplification of *CCND1* (28%)[8]. These alterations implicate the use of cell cycle inhibitors in OSCC. In recent years, cell cycle inhibitors with targeted activity towards specific components of the cell cycle have been developed and approved in a clinical setting for breast cancer[19,23]. Here, we describe the effects of the CDK4/6 inhibitor palbociclib on OSCC cell lines and tumor models. We found that majority of the OSCC cell lines responded to palbociclib treatment with concomitant reduction in RB phosphorylation, which resulted in inhibition of cell proliferation and G$_1$ cell cycle arrest. The *in vitro* observations were confirmed by significant tumor control in subcutaneous mouse models. A recent Phase I clinical trial on OSCC also reported tumor response in patients with OSCC treated with palbociclib, including those previously resistant to cetuximab or cisplatin[11], strongly

suggesting that palbociclib could be a promising therapeutic drug for patients with OSCC.

Understanding the molecular changes that could influence therapeutic response is vital for identifying subgroups that are most likely to benefit from palbociclib treatment. We leveraged on genomic information on well-characterized cell lines[12,18,24] and showed that *PIK3CA* mutations are associated with the resistance of OSCC cell lines to palbociclib. Using CAL27 isogenic cell lines, we confirmed that mutations in *PIK3CA* indeed confer resistance to palbociclib and other clinically approved CDK4/6 inhibitors. In *PIK3CA* mutant cell lines, this resistance is accompanied by an increase in cyclin E and CDK2 expression. *PIK3CA* mutations have been shown to increase the expression of cyclins and their dependent kinases. For example, in a non-tumorigenic human breast epithelial cell line, *PIK3CA* mutations resulted in the upregulation of cyclin D1, resulting in an increase in cell proliferation[25]. Furthermore, upregulation of cyclin D1 and CDK2-dependent Rb phosphorylation by PI3K activation was also reported in MCF7 cells in response to CDK4/6 inhibition[16]. *PIK3CA* mutations were also previously reported to increase cyclin E expression, where PI3K-dependent upregulation of cyclin E1 levels was associated with acquired resistance to CDK4/6 inhibition in pancreatic ductal adenocarcinoma[26]. PI3K activation can drive the cell cycle by regulating the expression of cell cycle inhibitors, including p21 and p27, as reported previously[27-29]. Furthermore, *PIK3CA* mutations could directly regulate cyclin D levels by inhibiting glycogen synthase kinase-3β expression, resulting in the stabilization and localization of cyclin D1 to the nucleus[25,30]. Based on our observation that activation of PI3K confers resistance to palbociclib, we demonstrated that treatment with a combination of palbociclib and a PI3K/mTOR inhibitor resulted in complete tumor growth control in the animal model. While PI3K/mTOR inhibition alone was also able to delay tumor growth, it was obvious that blocking PI3K signaling restored sensitivity to palbociclib in OSCC models. Concurring with our *in vitro* observations, complete tumor growth control was observed concomitantly with reduction in cyclin E1 and CDK2 expression. This is consistent with data from other studies where PI3K/mTOR inhibitor synergistically cooperated with CDK4/6 inhibitor in suppressing cell proliferation by reducing the levels of critical cell cycle regulatory proteins, such as cyclin E1, cyclin D1, CDK2, and cyclin A[26,31,32].

In summary, we demonstrated that palbociclib is effective in controlling tumor growth in most OSCC cell lines. Our data also revealed that *PIK3CA* mutational status may serve

as a biomarker for response to palbociclib and other clinically approved CDK4/6 inhibitors. Finally, we demonstrated that simultaneous inhibition of PI3K/mTOR and CDK4/6 is effective in controlling tumor growth in resistant OSCC cell lines. Given that clinical studies on CDK4/6 inhibitors in OSCC have been initiated, our study provides a rationale for testing biomarkers of response and suggests possible combinatorial approaches for patients who may not respond to CDK4/6 inhibitors as single agents.

Acknowledgements

Conflict of interest statement

No potential conflicts of interest are disclosed.

References

1. Torre LA, Bray F, Siegel RL, Ferlay J, Lortet-Tieulent J, Jemal A. Global cancer statistics, 2012. CA Cancer J Clin. 2015; 65: 87-108.

2. Warnakulasuriya S. Global epidemiology of oral and oropharyngeal cancer. Oral Oncol. 2009; 45: 309-16.

3. Rogers SN, Vedpathak SV, Lowe D. Reasons for delayed presentation in oral and oropharyngeal cancer: the patients perspective. Br J Oral Maxillofac Surg. 2011; 49: 349-53.

4. Edwards DM, Jones J. Incidence of and survival from upper aerodigestive tract cancers in the U.K.: the influence of deprivation. Eur. J. Cancer. 1999; 35: 968-72.

5. Vermorken JB, Mesia R, Rivera F, Remenar E, Kawecki A, Rottey S, et al. Platinum-based chemotherapy plus cetuximab in head and neck cancer. New Engl J Med. 2008; 359: 1116-27.

6. Rampias T, Giagini A, Siolos S, Matsuzaki H, Sasaki C, Scorilas A, et al. RAS/PI3K crosstalk and cetuximab resistance in head and neck squamous cell carcinoma. Clin Cancer Res. 2014; 20: 2933-46.

7. Chow LQ, Haddad R, Gupta S, Mahipal A, Mehra R, Tahara M, et al. Antitumor activity of pembrolizumab in biomarker-unselected patients with recurrent and/or metastatic head and neck squamous cell carcinoma: results from the phase Ib KEYNOTE-012 expansion cohort. J Clin Oncol. 2016; 34: 3838-45.

8. Cancer Genome Atlas Network. Comprehensive genomic characterization of head and neck squamous cell carcinomas. Nature. 2015; 517: 576-82.

9. Finn RS, Crown JP, Lang I, Boer K, Bondarenko IM, Kulyk SO, et al. The cyclin-dependent kinase 4/6 inhibitor palbociclib in combination with letrozole versus letrozole alone as first-line treatment of oestrogen receptor-positive, HER2-negative, advanced breast cancer (PALOMA-1/TRIO-18): a randomised phase 2 study. Lancet Oncol. 2015; 16: 25-35.

10. Cristofanilli M, Turner NC, Bondarenko I, Ro J, Im SA, Masuda N, et al. Fulvestrant plus palbociclib versus fulvestrant plus placebo for treatment of hormone-receptor-positive, HER2-negative metastatic breast cancer that progressed on previous endocrine therapy (PALOMA-3): final analysis of the multicentre, double-blind, phase 3 randomised controlled trial. Lancet Oncol. 2016; 17: 425-39.

11. Michel L, Ley J, Wildes TM, Schaffer A, Robinson A, Chun SE, et al. Phase I trial of palbociclib, a selective cyclin dependent kinase 4/6 inhibitor, in combination with cetuximab in patients with recurrent/metastatic head and neck squamous cell carcinoma. Oral Oncol. 2016; 58: 41-8.

12. Fadlullah MZH, Chiang IKN, Dionne KR, Yee PS, Gan CP, Sam KK, et al. Genetically-defined novel oral squamous cell carcinoma cell lines for the development of molecular therapies. Oncotarget. 2016; 7: 27802-18.

13. Hamid S, Lim KP, Zain RB, Ismail SM, Lau SH, Mustafa WMW, et al. Establishment and characterization of Asian oral cancer cell lines as *in vitro* models to study a disease prevalent in Asia. Int J Mol Med. 2007; 19: 453-60.

14. Wang ZY, Martin D, Molinolo AA, Patel V, Iglesias-Bartolome R, Degese MS, et al. Mtor Co-targeting in cetuximab resistance in head and neck cancers harboring *PIK3CA* and *RAS* mutations. J Natl Cancer Inst. 2014; 106: dju215.

15. Zarkowska T, Mittnacht S. Differential phosphorylation of the retinoblastoma protein by G_1/S cyclin-dependent kinases. J Biol Chem. 1997; 272: 12738-46.

16. Herrera-Abreu MT, Palafox M, Asghar U, Rivas MA, Cutts RJ, Garcia-Murillas I, et al. Early adaptation and acquired resistance to CDK4/6 inhibition in estrogen receptor-positive breast cancer. Cancer Res. 2016; 76: 2301-13.

17. Li CS, Qi L, Bellail AC, Hao CH, Liu TJ. PD-0332991 induces G1 arrest of colorectal carcinoma cells through inhibition of the cyclin-dependent kinase-6 and retinoblastoma protein axis. Oncol Lett. 2014; 7: 1673-8.

18. Lee BKB, Gan CP, Chang JK, Tan JL, Fadlullah MZ, Abdul Rahman ZA, et al. Genipac: a genomic information portal for head and neck cancer cell systems. J Dent Res. 2018; 97: 909-16.

19. O'Shaughnessy J, Petrakova K, Sonke GS, Conte P, Arteaga CL, Cameron DA, et al. Ribociclib plus letrozole versus letrozole alone in patients with de novo HR+, HER2− advanced breast cancer in the randomized monaleesa-2 trial. Breast Cancer Res Treat. 2018; 168: 127-34.

20. Sledge GW Jr, Toi M, Neven P, Sohn J, Inoue K, Pivot X, et al. Monarch 2: abemaciclib in combination with fulvestrant in women with HR+/HER2- advanced breast cancer who had progressed while receiving endocrine therapy. J Clin Oncol. 2017; 35: 2875-84.

21. Schmitz NMR, Hirt A, Aebi M, Leibundgut K. Limited redundancy in phosphorylation of retinoblastoma tumor suppressor protein by cyclin-dependent kinases in acute lymphoblastic leukemia. Am J Pathol. 2006; 169: 1074-9.

22. Kitagawa M, Higashi H, Jung HK, Suzuki-Takahashi I, Ikeda M,

Tamai K, et al. The consensus motif for phosphorylation by cyclin D1-Cdk4 is different from that for phosphorylation by cyclin A/E-Cdk2. EMBO J. 1996; 15: 7060-9.

23.   Finn RS, Martin M, Rugo HS, Jones SE, Im SA, Gelmon KA, et al. Paloma-2: primary results from a phase III trial of palbociclib (P) with letrozole (L) compared with letrozole alone in postmenopausal women with ER+/HER2-advanced breast cancer (ABC). J Clin Oncol. 2016; 34: 507.

24.   Martin D, Abba MC, Molinolo AA, Vitale-Cross L, Wang ZY, Zaida M, et al. The head and neck cancer cell oncogenome: a platform for the development of precision molecular therapies. Oncotarget. 2014; 5: 8906-23.

25.   Gustin JP, Karakas B, Weiss MB, Abukhdeir AM, Lauring J, Garay JP, et al. Knockin of mutant *PIK3CA* activates multiple oncogenic pathways. Proc Natl Acad Sci USA. 2009; 106: 2835-40.

26.   Franco J, Witkiewicz AK, Knudsen ES. CDK4/6 inhibitors have potent activity in combination with pathway selective therapeutic agents in models of pancreatic cancer. Oncotarget. 2014; 5: 6512-25.

27.   Medema RH, Kops GJPL, Bos JL, Burgering BMT. AFX-like forkhead transcription factors mediate cell-cycle regulation by Ras and PKB through p27[Kip1]. Nature. 2000; 404: 782-7.

28.   Graff JR, Konicek BW, McNulty AM, Wang ZJ, Houck K, Allen S, et al. Increased akt activity contributes to prostate cancer progression by dramatically accelerating prostate tumor growth and diminishing p27[Kip1] expression. J Biol Chem. 2000; 275: 24500-5.

29.   Samuels Y, Diaz LA Jr, Schmidt-Kittler O, Cummins JM, DeLong L, Cheong I, et al. Mutant *PIK3CA* promotes cell growth and invasion of human cancer cells. Cancer Cell. 2005; 7: 561-73.

30.   Diehl JA, Cheng MG, Roussel MF, Sherr CJ. Glycogen synthase kinase-3β regulates cyclin D1 proteolysis and subcellular localization. Genes Dev. 1998; 12: 3499-511.

31.   Bonelli MA, Digiacomo G, Fumarola C, Alfieri R, Quaini F, Falco A, et al. Combined inhibition of CDK4/6 and PI3K/AKT/mTOR pathways induces a synergistic anti-tumor effect in malignant pleural mesothelioma cells. Neoplasia. 2017; 19: 637-48.

32.   O'Brien NA, Tomaso ED, Ayala R, Tong L, Issakhanian S, Linnartz R, et al. *In vivo* efficacy of combined targeting of CDK4/6, ER and PI3K signaling in ER+ breast cancer. Cancer Res. 2014; 74: 4756.
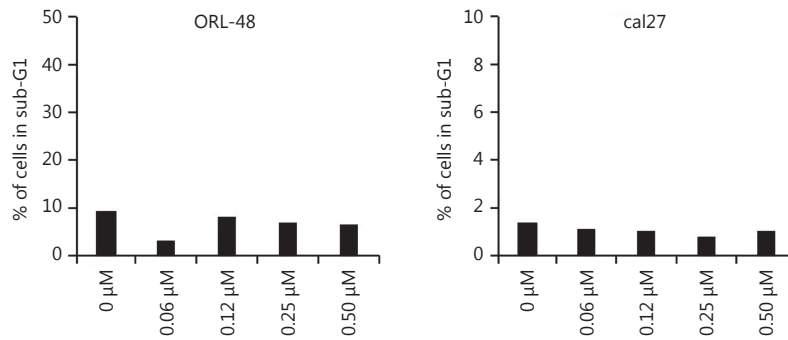
Supplementary materials

Figure S1 Escalating dose of palbociclib (24 h) did not change the sub-G$_1$ cell population in CAL27 and ORL-48 cells by propidium iodide analysis.
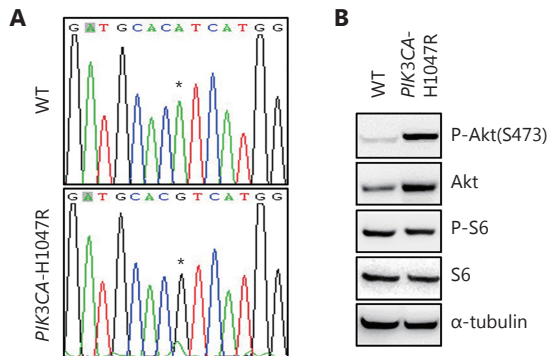

Figure S2 CAL27 cells were previously engineered to stably express *PIK3CA* (H1047R) alteration through retroviral infection. (A) DNA chromatogram of WT and mutant CAL27 cells confirmed base substitution from A (wild type; WT) to G (mutant) resulting in the change of amino acid R at position 1047. (B) Proteins extracted from mutant CAL27 cells showed over-activation of Akt (S473) but not in WT CAL27 cells by western blotting.